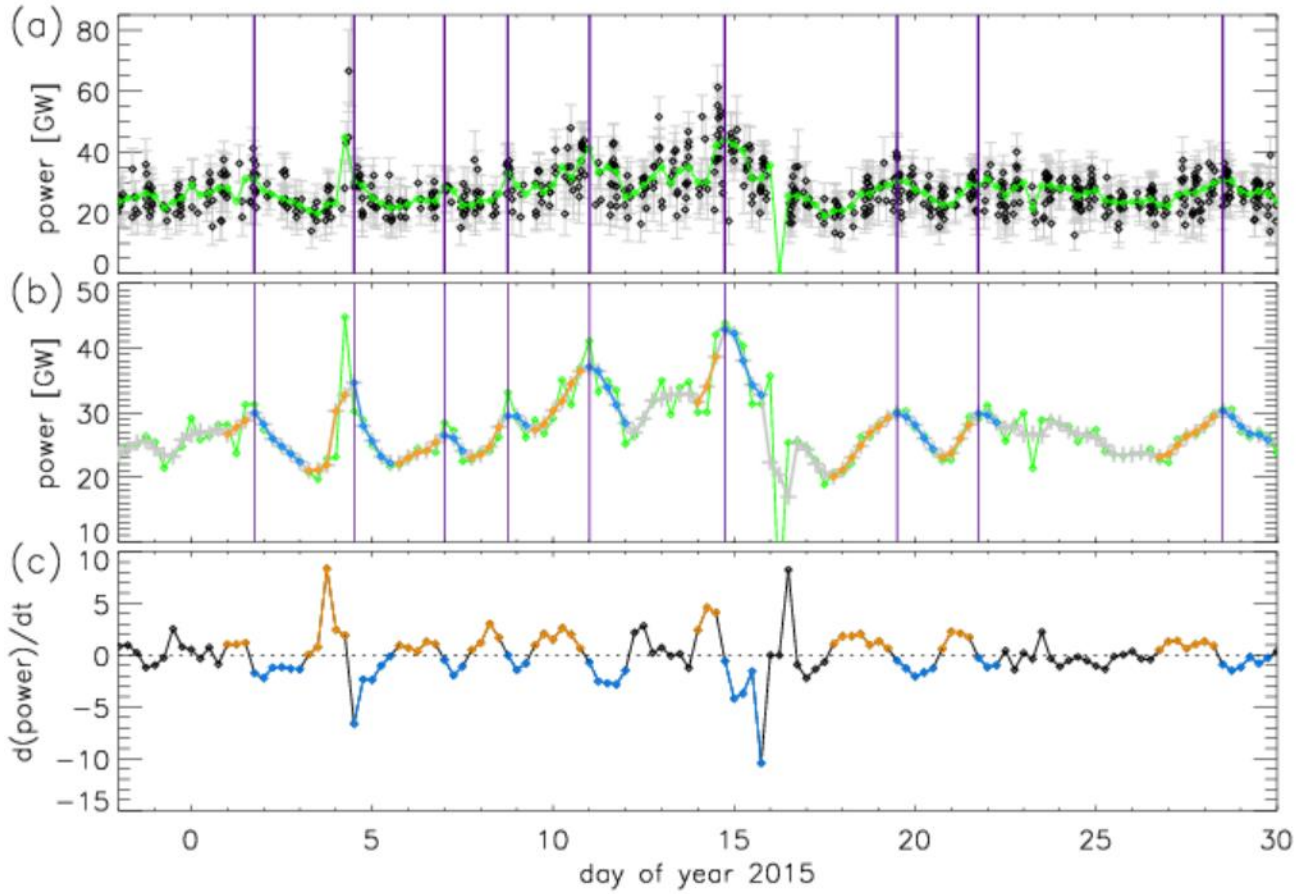

Figure 1. Time variations of (a) the auroral power emitted at wavelengths of 138.5–144.8 nm (black diamonds) and its median within the 0.5-day window shifted by 0.25 day (green line), (b) the same median power (green) and its 0.75-day (3-point) running average (grey line), and (c) time deviation of the power from December 29, 2014 to January 30, 2015. The detected positive and negative intervals continuing for ≥0.5 day are shown by orange and blue colours, respectively, in Figures 1b and 1c. Grey vertical lines in Figures 1a show errors estimated from the photon statistics. Purple vertical lines in Figures 1a and 1b represent the peak time of the quasi-periodic event detected automatically.

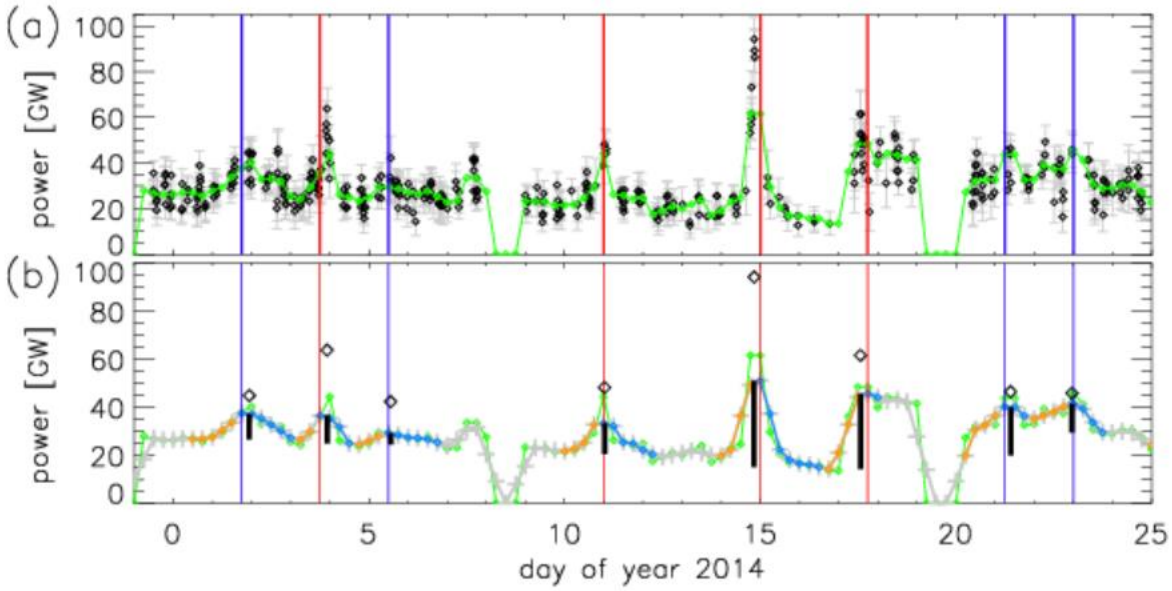

Figure 2. As Figures 1a and 1b but from December 30, 2013 to January 24, 2014. The black vertical lines in Figure 2b show the detected amplitudes of the periodic variation, and diamonds show the largest power during each enhancement. Red and blue lines represent the existence and absence of significant auroral enhancement, respectively.

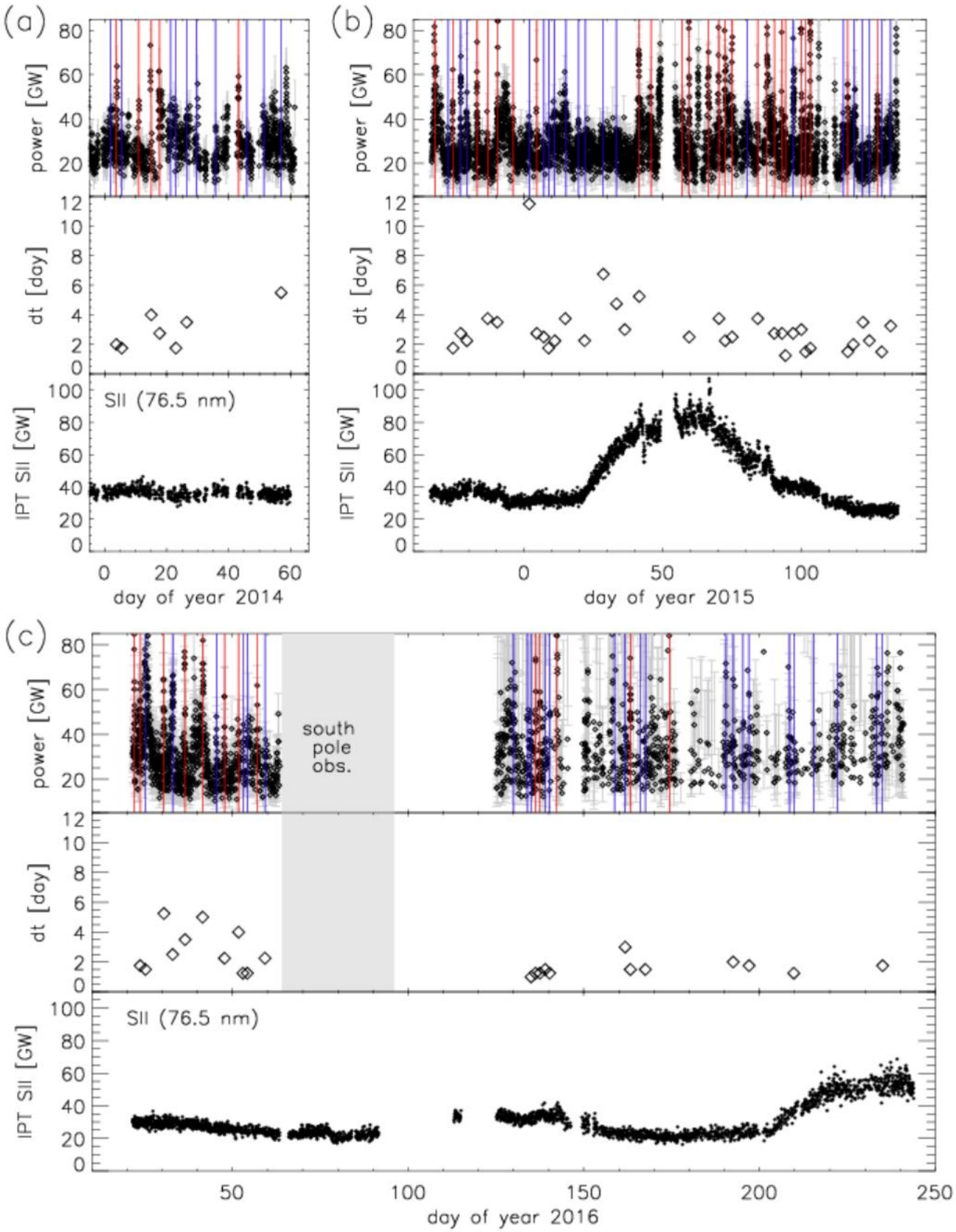

Figure 3. Time variations of the power emitted at wavelengths of 138.5–144.8 nm (upper), interval of events dt (middle), and IPT SII emission intensity (bottom, see Yoshikawa et al., 2017 for details) , observed in (a) 2014, (b) 2015, and (c) 2016. Grey vertical lines in the upper plots show errors estimated from the photon statistics, and red and blue vertical lines represent the peak times of periodic events with and without significant enhancement, respectively.

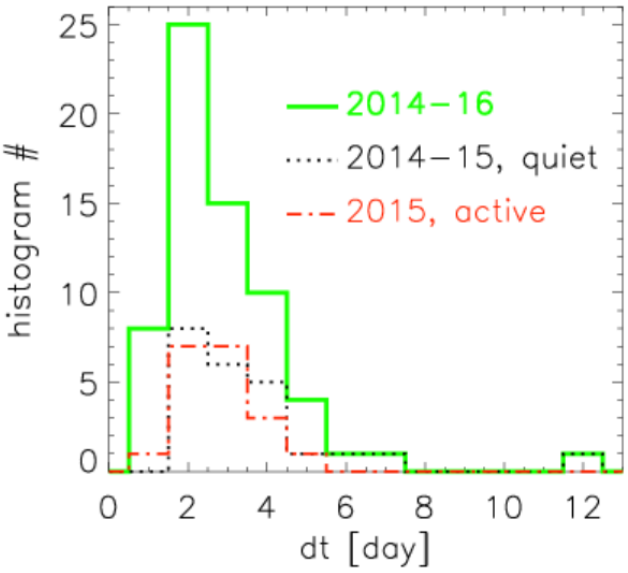

Figure 4. Histogram of separation interval *dt* of periodic events for all the 2014–2016 dataset (green line), Io's volcanically quiet time in 2014–2015 (black dotted line), and Io's volcanically active time in 2015 (red dot-dashed line).

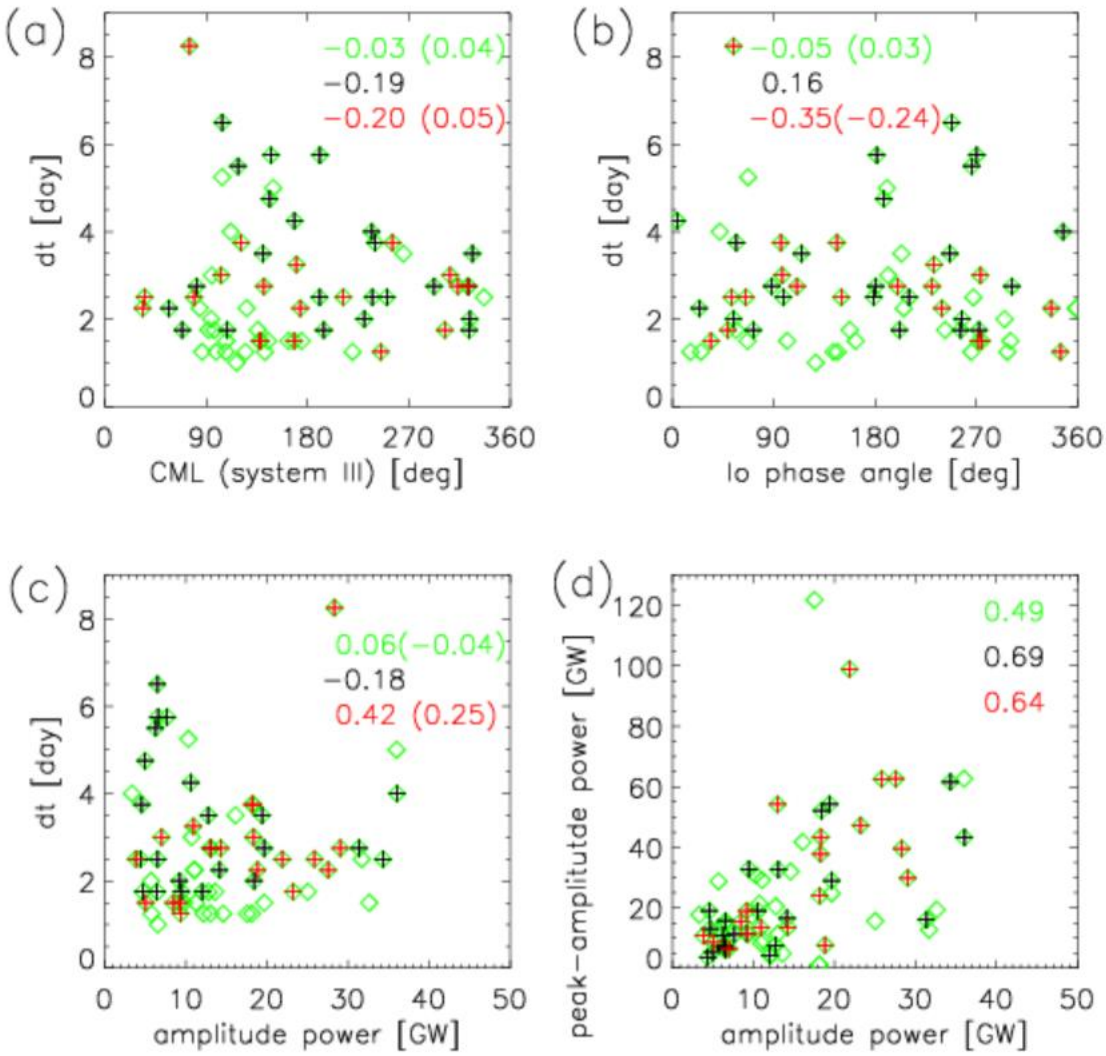

Figure 5. Separation interval *dt* as a function of (a) CML, (b) Io phase angle, and (c) amplitude power of the periodic variation, and (d) correlation between amplitude power and peak-amplitude power, for all the dataset over 2014–2016 (green diamonds), Io's volcanically quiet time (black pluses), and volcanically active time (red pluses). Numbers in the upper part of each plot are the correlation coefficient, and those in brackets are the correlation coefficients excluding the extreme case with *dt* > 8 days.

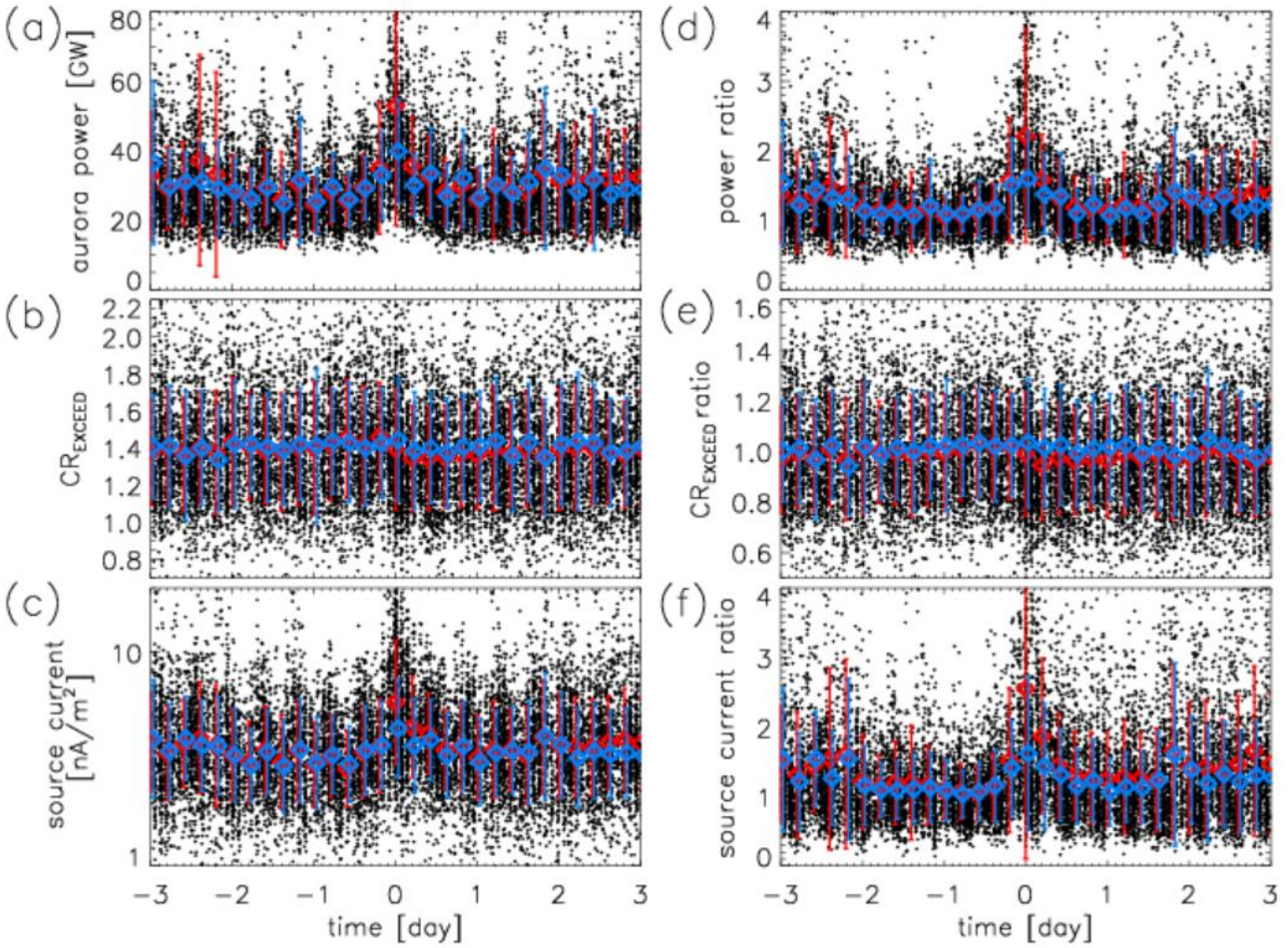

Figure 6. Results of superposed-epoch analysis for the periodic events showing (a) auroral power at 138.5–144.8 nm with rotational modulation correction, (b) CR_{EXCEED}, and (c) maximum field-aligned current that can be carried by precipitating magnetospheric electrons without field-aligned acceleration, and superposed-epoch analysis showing relative increase (see detail in text) of (d) auroral power, (e) CR_{EXCEED}, and (f) field-aligned current. The mean value within each 0.2-day bin for all events and that for events without bursts are shown by red and blue diamonds, respectively, with error bars showing the variance.

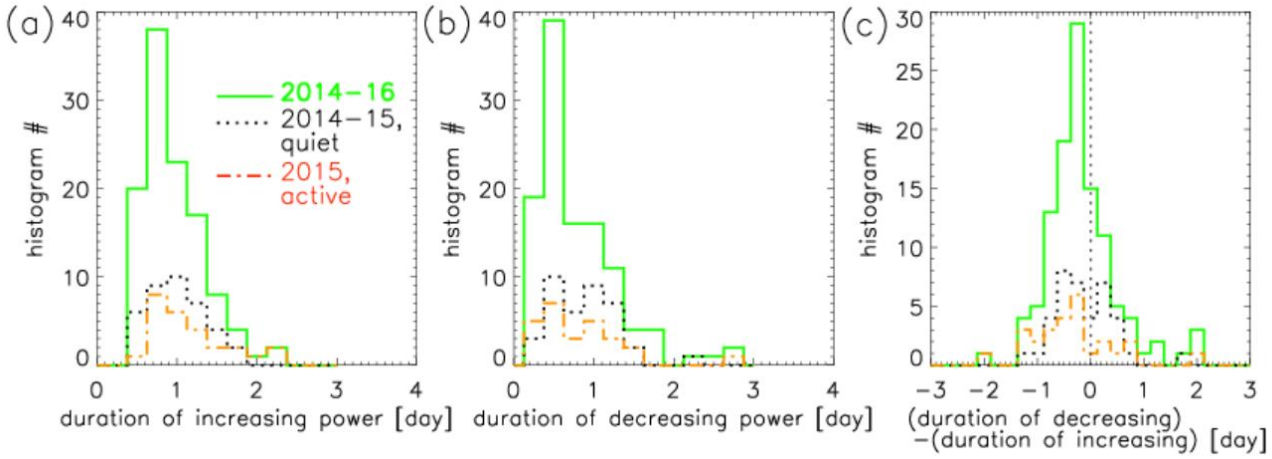

Figure 7. Histogram for the (a) durations of increasing power, (b) decreasing power, and (c) their difference in periodic events for the entire 2014–2016 dataset (solid green line), Io's volcanic quiet time in 2014–2015 (black dotted line), and Io's volcanic active time in 2015 (orange dot-dashed line).

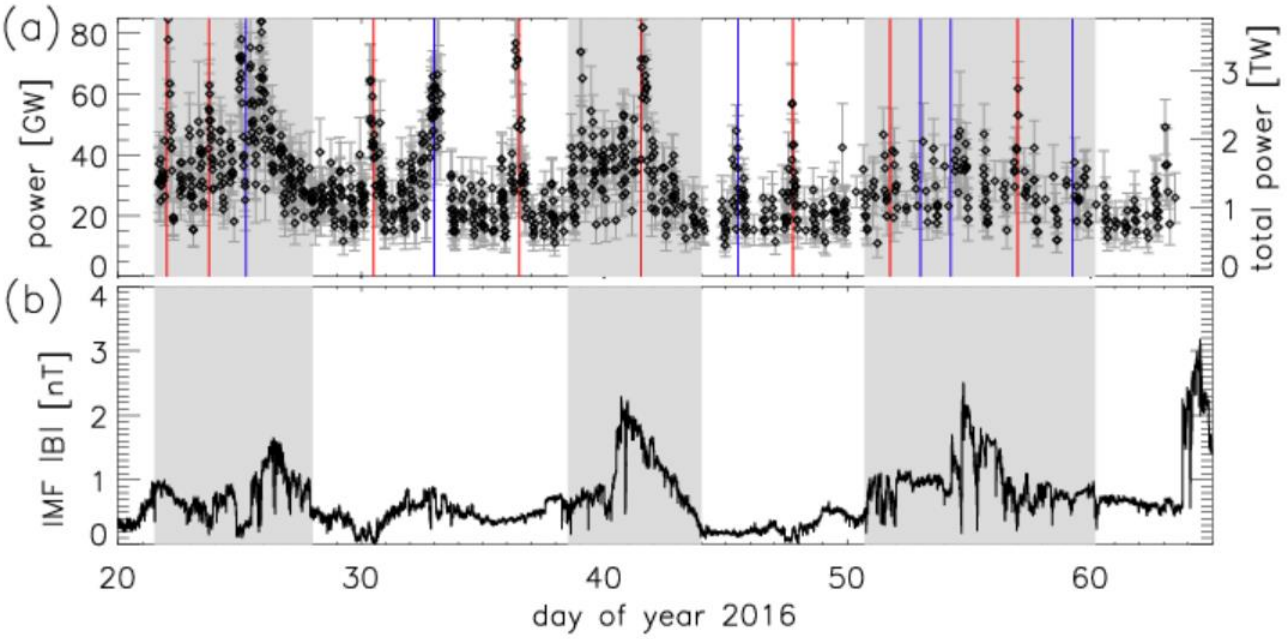

Figure 8. Time variations of (a) auroral powers emitted at wavelengths of 138.5–144.8 nm and (b) interplanetary magnetic field strength observed by Juno for DOY 20–64 in 2016. In Figure 8a, grey vertical lines show errors estimated from the photon statistics, and red and blue vertical lines represent the peak times of periodic events with and without auroral bursts, respectively. The right y-axis in Figure 8a shows the auroral power over wavelengths of 80–170 nm without absorption. Grey hatched regions are solar wind events.

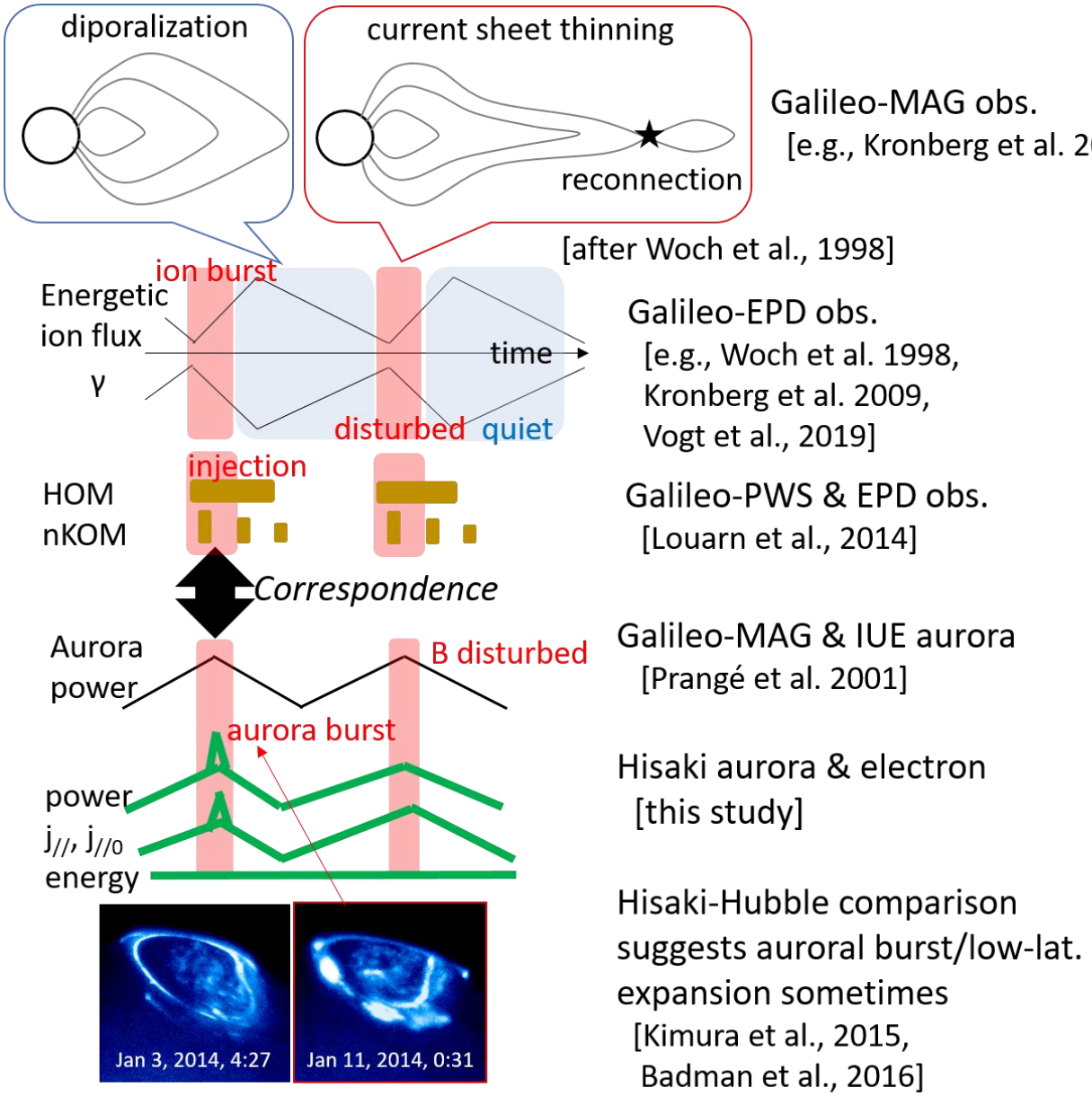

Figure 9. Schematics representing from top to bottom the magnetospheric reconfiguration model and the related observed characteristics of the energetic ion flux and spectral index γ; the auroral radio emissions; the auroral power from previous observation; the auroral power, flux, and energy from this study; and auroral images taken by HST at quiet (left) and disturbed (right) times.

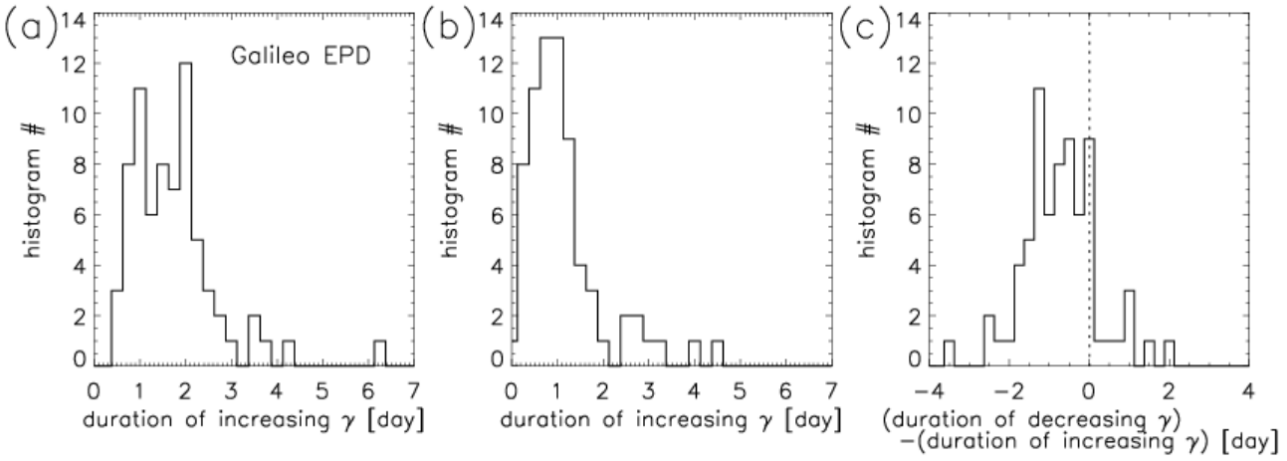

Figure 10. Histograms for the (a) durations of increasing and (b) decreasing spectral index γ of energetic ion distributions and (c) their difference observed by the Galileo EPD.